



Research article

Prediction and Optimization of Roadheader Performance based on Characteristics and Geo-Mechanical Parameters of Rock (Case Study: TABAS Parvedeh coal mine No. 1)

Amin Faramarz¹, Gholamreaz Saeedi^{2*}, Ali Hosseini³, Sajjad Aghababaei²

- 1- Dept. of Mining Engineering, Zarand Higher Education Complex, Shahid Bahonar University of Kerman, Kerman, Iran
- 2- Dept. of Mining Engineering, Faculty of Engineering and Technology, Shahid Bahonar University of Kerman, Kerman, Iran
- 3- Dept. of Mining and Metallurgy Engineering, Yazd University, Yazd, Iran

*Corresponding author: E-mail: gsaeedi@uk.ac.ir

(Received: February 2024, Accepted: September 2025)

DOI: [10.22034/ANM.2025.21296.1628](https://doi.org/10.22034/ANM.2025.21296.1628)

Keywords	Abstract
Performance prediction	Roadheader machines have good efficiency and flexibility in mechanized tunneling and underground mining. The application of Roadheaders increases the speed of excavation in the tunnels, which dramatically reduces the time and cost of the project. Considering the importance of this issue, this study aims to predict and optimize the penetration rate and excavation speed of Roadheaders using the particle swarm algorithm in Parvadeh No. 1 mechanized coal mine.
Roadheader	
Nonlinear and linear regression	
Coal mine	
Particle Swarm Optimization	
Therefore, in this study, the characteristics of Roadheaders have been investigated in related studies. All of these studies were divided into two parts: field observations and laboratory tests. In this research, tunnel number one is considered as the case study, which is divided into 30 parts/sections, and in each section, rock core/sample preparation, the number of joints along the tunnel, excavation time, and volume of the excavated rock mass under the Roadheader machine operation were measured. In the laboratory studies section, the rock core was analyzed by the uniaxial compression strength (UCS) test, and finally, a database was provided based on the obtained results. In the following, nonlinear and linear regression models were used to select the best model for estimating the instantaneous cutting rate (ICR) of the Roadheader machine, which expresses the advancing rate of excavation. In these models, parameters including rock quality designation (RQD) of rock mass, tensile strength (σ_t), UCS, rock mass brittleness index (RMBI), pick consumption index (PCI), pick consumption factor (PCf), and specific energy (SE) were selected as input variables, and ICR was selected as the output variable. By comparing the results, the linear regression model had the highest determination coefficient and performance index, and the lowest root mean square error. Therefore, this model was selected as the most suitable model. In order to optimize ICR, the relationship obtained from the linear regression model was implemented in the particle swarm algorithm. The results showed that to obtain the optimal limit of ICR in the considered case study with a UCS of 1.68 MPa and a RQD of 33.09%, ICR is equal to 33.11 cubic meters per hour.	

1. INTRODUCTION

Mechanized tunneling systems can be a suitable alternative to the traditional method of

mining operations because they can be performed more precisely and faster at a lower cost, and produce more productive output [1]. In addition,

with the application of the mechanized method, the maintenance and the required manpower are reduced. Due to new developments and enhancements to increase the performance and reliability of drilling machines, miners who use mechanized excavation systems have a larger share of the mineral products market [2, 3]. Some of the more important factors in mechanized excavation are the prediction of costs and completion time of the project, which depend on the performance of the machine and its efficiency. Predicting the performance of the machine will have a direct effect on the speed of production and ultimately the profitability of excavation projects [4, 5].

Generally, the factors affecting the performance of excavation operations can be classified into four main categories which are described in the following.

A- Rock material parameters consist of compressive and tensile strength, hardness percent, abrasive minerals (quartz), type of texture and matrix of rock, elastic behavior, and rock energy properties such as rigidity index

B- Rock mass parameters such as the joint inclination, joint spacing, direction of discontinuities, junctions, groundwater, fault areas, position of the frontier, general classification of the rockmass, maintenance requirements, and field stress [6, 7].

C- Machine characteristics, including weight, power, machine forces, type of drum cutter, arrangement of cutting tools, and support system capacity.

D- Operation parameters consisting of shape, size, inclination, and length of excavation, path arc, drilling arrangement, acceleration operations, number of rock formations in the tunnel path, site management method, and work scheduling, which is the number of work shifts per day [8-11].

A combination of these parameters specifies the speed of excavation operation and the capacity of the machine production in a rockmass [12]. In this research, we attempt to present a model predicting the performance of a Roadheader based on geomechanically parameters of rock and drilling machine characteristics in a fully mechanized coal mine in Parvadeh No. 1 mine.

2. GENERAL STATUS AND CHARACTERISTICS OF PARVADEH NO. 1 COAL MINE OF TABAS

Tabas's city is located in the northeast of Yazd Province, Iran. Figure 1 shows the plan of Parvadeh No. 1. The thickness of the main coal zone is approximately 100 m, including five coal seams called B1, B2, C1, C2, and D which have the

applicable thickness. Among these layers, the three layers C1, B2, and B1 are extractable economically. Coal seams are accessed by four diagonal tunnels with an inclination of 14 degrees. The mechanized longitudinal longwall method is used to extract the coal seams. In this mine, the Roadheader machine has been applied to develop the excavations such as roadways, slopes, cross-cuts [13, 14].

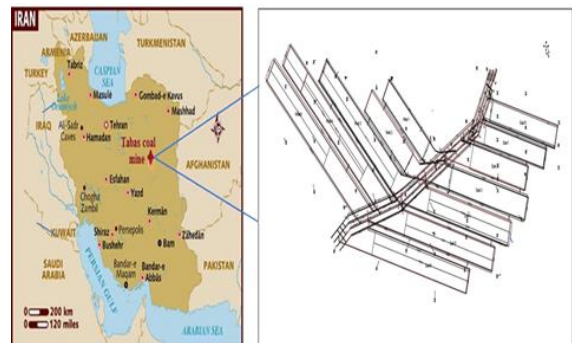


Fig. 1. The Tabas Parvadeh No. 1 coal mine [14].

In tunnel No.1 of the mine, four road-header machines were used excavation operation (Fig. 2). The model of these machines is DOSCO MD1100. It should be noted that in this mine, drilling and blasting systems are used in the conditions of existing hard rock formations (sandstone). The Roadheader machine is ranked among the lightweight to medium-weight machines. According to the application levels in British charcoal mines, this Roadheader is an ideal device for the extraction of mixed layers. Table 1 shows the main characteristics of the machine. [15, 16].



Fig. 2. A view of the Roadheader machine with axial excavation method in coal mines of Tabas [17].

Table 1. Observation performed in 30 tunnel sections

Roadheader characteristics	Unit	Value
Car length	mm	8066
Main body height of the machine	mm	1860
Body width of the machine	mm	2500
Boom rotation angle	degree	45
Cutting height maximum	mm	4700
Cutting width maximum	m	6160
Machine weight	ton	34
Cutting slice speed	rpm	32-58
Movement speed	m per sec	1.18
Conveyor width	mm	615

3. INVESTIGATING THE PERFORMANCE OF ROADHEADER MACHINE

Road headers are generally suitable for low to medium-strength rocks. There is no direct relationship between the machine and the tunnel shape. The cross-section of the tunnel excavated using this machine can be different. The tunnel surface is directly available at any time because these machines directly affect the bottom of the tunnel; it should have sufficient load capacity [18, 19].

Researchers have developed a lot of relationships to determine the infiltration rate of Roadheaders. Bilgin and colleagues presented Eq. (1) for the instantaneous cutting rate (ICR) for various transverse and axial Roadheaders [1].

$$ICR = 9.07 \ln(RMBI) + 29.93 \quad (1)$$

where RMBI is the Rock mass brittleness index. This is calculated by Eq. (2) [1].

$$RMBI = e^{\left(\frac{\sigma_c}{\sigma_t}\right)} \times \left(\frac{RQD}{100}\right)^3 \quad (2)$$

In Eq. (2), σ_c is uniaxial compressive strength of intact rock; σ_t is the tensile strength of the intact rock, and RQD is the rock quality designation of rockmass. RQD of the rock mass is one of the most important factors affecting the performance of the Roadheader. In this study, this parameter is evaluated by Eq. (3) presented by Prest and Hudson [22].

$$RQD = 100e^{-0.1\lambda}(0.1\lambda + 1) \quad (3)$$

In Eq. (3), λ is the number of joints along the excavation strike/line. Using RMBI, we can calculate the pick consumption index (PCI) of Roadheader as the Eq. (4) [1].

$$PCI = e^{RMBI} \times \left(\frac{UCS}{P}\right) \quad (4)$$

In Eq. (4), UCS is the uniaxial compressive strength of the rock and P is the power of the digger, which is equal 84 KW. The pick consumption factor is a function (PCF) of PCI, which is calculated by Eq. (5) [1].

$$PCF = 45.67(PCI)^{-0.16} \quad (5)$$

The specific energy (SE) for the Roadheader is a function of σ_c , which can be calculated by the following equation: [1].

$$SE = 0.123\sigma_c + 0.97 \quad (6)$$

4. PSO ALGORITHM (PARTICLE SWARM OPTIMIZATION)

PSO (Particle Swarm Optimization) is an optimization method that can be used to deal with problems whose answers are a point or a surface in n-dimensional space. In this space, the assumptions are discussed, an initial speed is allocated to them, and communication channels are considered between particles. Then, these particles move in the space of the reaction, and the results are calculated based on a merit criterion after each period. Over time, particles tend to accelerate toward particles with a higher degree of merit and are in the same communication group. Despite the fact that every method works well in a range of issues, this method has been successful in solving continuous optimization problems. Using this algorithm, we can optimize the Roadheader progress rate [21]. There are four steps for PSO algorithm, which are mentioned in the following:

- (1) Creating a critical mass and evaluating it;
- (2) Determining the best personal memories and the best collective memories;
- (3) Updating the speed and position;
- (4) If the stop conditions are not met, go to step 1 otherwise, it will end.

The termination conditions of this algorithm are as follows:

- 1) To reach an acceptable response rate,
- 2) The number of repetitions,
- 3) The number of repetitions passed without a certain improvement in the result, and
- 4) Completing a certain number of responses [18].

Particle deformation in this algorithm is based on the experience of the particles and the rest of the particles. Particles tend to experience the best

position and direction that they themselves or other neighbors have taken in the past. In general, it can be stated that the behavior and position of the rest of the particles on the hair are influenced by a small particle to achieve successful particles. Modeling PSO is also based on the search for successful particle swarming points, which has transformed PSO into a social search algorithm [19].

Particles attempt to gain the best position in the search space with respect to the memory of their experiences and knowledge and their collective intelligence. Particles compete to gain the best position over the rest of their neighbors [19].

5. DATA COLLECTION

Database was created based on the data collected through the field and the laboratory, which are described in the following:

A- Field observations: In this section, the tunnel considered as the case study was divided into 30 parts along the tunnel strike and in each section, the rock core sampling work was carried out using a machine tool. In each section, three rock cores with a diameter of 54 mm were drilled. Simultaneously, the number of joints in the tunnel was counted along a withdrawal line. The number of joints in these 30 sections recorded between 22 to 26. During the Roadheader operation, the time and volume were also measured for excavating each section (Table 2).

B- Laboratory tests: The rock cores drilled in the tunnel were examined in the laboratory under a point load test to calculate the UCS and tensile strength. The height of the rock samples was 27–53 mm, and their diameter was 54 mm in all tests.

Many methods can be used to obtain tensile and compressive strength, one of which is the use of a point test. Point load testing is performed on small pieces of rock called cores[21]. Based on the described process to create the database, the required data was collected. In this regard, data about parameters, including the type of rock, excavating volume, time, number of joints per unit length, and RQD are presented in Table 2. Table 3 illustrates the data of point load index, compressive strength, and tensile strength of the rock. In the following, the amounts of RMBI, PCI, PCF, SE, and ICR were determined and the results are presented in (Table 4).

Table 2. Observation performed in 30 tunnel sections

excavating ring	Type of rock	excavating volume (m ³)	time (min)	Number of joints per unit length (λ)	RQD%
1	Argillite	23.4	60	25	28.73
2	Silt-stone	22.5	54	24	30.84
3	Silt-stone	22.8	89	20	40.60
4	Argillite	25	49	22	35.46
5	Argillite	24.6	81	25	28.73
6	Argillite	25.2	57	24	30.84
7	Silt-stone	22.6	70	24	30.84
8	Silt-stone	22.7	62	22	35.46
9	Silt-stone	23.2	69	24	30.84
10	Argillite	26.4	64	24	30.84
11	Silt-stone	22.9	86	23	33.09
12	Silt-stone	22.4	45	23	33.09
13	Silt-stone	23.1	67	22	35.46
14	Silt-stone	24.2	56	20	40.60
15	Argillite	25.7	58	22	35.46
16	Argillite	24.9	38	22	35.46
17	Argillite	26.1	67	25	28.73
18	Silt-stone	23.2	65	24	30.84
19	Silt-stone	23.7	54	20	28.73
20	Coal	29.9	62	26	26.74
21	Silt-stone	24.2	74	23	33.09
22	Silt-stone	23.8	80	24	30.84
23	Silt-stone	26.1	39	20	40.60
24	Coal	28.4	55	26	26.74
25	Silt-stone	22.3	69	23	33.09
26	Silt-stone	22.9	73	23	33.09
27	Argillite	25.6	49	25	28.73
28	Argillite	26.7	52	24	30.84
29	Silt-stone	23	67	22	35.46
30	Silt-stone	22.8	82	22	35.46

Table 3. Calculations of the point load index, compressive resistance and tensile resistance of samples

Samples	Suitable load to break sample (kN)	Diameter (mm)	Point load index (MPa)	Is (50) (MPa)	Compressive resistance of sample (MPa)	Tensile resistance of sample (MPa)	Correction factor
1	4.20	43.10	2.26	2.11	50.73	2.03	0.94
2	4.90	43.65	2.15	2.10	50.49	2.02	0.98
3	20.89	46.92	2.22	2.16	51.78	2.07	1.07
4	5.11	58.65	1.48	1.59	38.16	1.53	1.09
5	5.02	55.64	1.62	1.70	40.79	1.63	0.99
6	4.73	49.07	1.95	1.93	51.63	2.07	0.94
7	4.12	43.10	2.30	2.15	51.19	2.05	1.02
8	4.93	52.46	1.79	1.83	43.90	1.76	0.96
9	4.74	46.18	2.22	2.14	51.41	2.06	0.94
10	4.31	43.89	2.23	2.10	50.47	2.02	0.95
11	4.37	44.66	2.19	2.08	49.97	2	1.03
12	5.01	53.75	1.73	1.79	42.89	1.72	1.04
13	5.05	55.02	1.66	1.73	41.59	1.66	1.01
14	5.01	51.13	1.91	1.93	46.30	1.85	1.07
15	5.21	58.06	1.54	1.65	39.53	1.58	0.95
16	4.33	44.66	2.17	2.06	49.50	1.98	0.96
17	4.55	45.43	2.20	2.11	50.57	2.02	1.08
18	5.99	59.81	1.67	1.81	43.44	1.74	1.04
19	5.81	55.02	1.92	2.00	48.11	1.92	0.94
20	3.01	43.10	2.18	2.04	48.94	1.96	1.00
21	4.45	50.45	1.74	1.75	41.93	1.68	1.00
22	4.33	79.67	1.74	1.74	41.67	1.67	1.62
23	5.02	54.39	1.6	1.76	42.12	1.68	1.04
24	3.02	43.10	1.99	1.86	44.67	1.79	0.94
25	6.01	60.38	1.64	1.79	42.85	1.71	1.09
26	4.02	44.66	2.01	1.91	45.85	1.83	0.95
27	4.34	51.80	1.61	1.64	39.26	1.57	1.02
28	3.99	43.89	2.07	1.95	36.85	1.87	0.94
29	4.01	46.18	1.88	1.81	43.53	1.74	0.96
30	5.23	53.11	1.85	1.90	45.62	1.82	1.03

Table 4. Calculation of the instantaneous drilling rate

Excavation section	Index fragility of rock mass (RMBI)	Partition consumption index (PCI)	Partition consumption factor (m ³ /pick)	Specific energy MJ/m ³	instantaneous drilling rate (m ³ /h)
1	1.69	3.27	37.78	7.21	34.79
2	2.1	4.91	35.41	7.18	36.66
3	4.88	81.14	22.60	7.34	44.31
4	3.02	9.31	31.96	5.66	39.95
5	1.47	2.11	40.52	5.99	33.42
6	2.01	4.59	35.79	7.32	36.26
7	2.05	4.73	35.61	7.27	36.44
8	3.03	1.82	31.20	6.37	39.98
9	2.02	4.61	35.76	7.29	36.31
10	2.08	4.81	35.52	7.18	36.57
11	2.55	7.62	33.00	7.12	38.42
12	2.44	5.86	34.42	6.25	38.02
13	3.38	14.54	29.76	6.09	40.98
14	4.95	77.81	22.75	6.66	44.44
15	3.2	12.38	30.53	5.83	40.68
16	1.76	14.46	29.79	7.06	40.48
17	2.04	3.50	37.38	7.19	35.06
18	1.8	3.98	36.62	6.31	36.40
19	1.36	3.46	37.44	6.89	35.26
20	2.5	2.27	40.06	6.99	32.72
21	2.04	6.08	34.21	6.13	38.24
22	5.17	3.82	36.86	6.10	36.40
23	1.3	88.21	22.30	6.15	44.83
24	2.76	1.95	41.04	6.46	32.31
25	2.75	8.06	32.71	6.24	39.14
26	2.71	8.54	32.40	6.61	39.11
27	1.22	2.58	39.23	5.80	34.80
28	2.26	5.14	35.15	6.73	37.16
29	3.42	13.50	30.11	6.32	40.65
30	1.69	16.60	29.13	6.58	41.08

6. STATISTICAL SURVEY OF THE VARIABLES

In this study, descriptive statistics were used to predict the instantaneous drilling rate of

inferential statistics (including correlation coefficient and multivariate regression). Descriptive statistics of considered variables/parameters are presented in Table 5.

Table 5. Descriptive statistics of all 30 excavated sections in the considered advancing tunnel

Number	Parameter	Indication	Mean	Minimum	Maximum	Standard deviation
1	instantaneous cutting rate	ICR	21.17	20.54	36.29	3.85
2	Rock quality designation	RQD	14.33	13.75	24.75	6.038
3	Tensile strength	σ_t	0.09	0.59	0.663	0.173
4	Uniaxial comprehensive strength	UCS	22.31	5.35	16.71	4.36
5	Rock mass brittleness index	RMBI	4.34	1.09	2.214	1.028
6	Pick consumption index	PCI	24.44	0.44	3.476	6.309
7	Pick consumption factor	PCF	57.34	26.71	42.76	6.8363
8	Specific energy	SE	2.95	1.33	3.210	0.52

7. PREDICTION OF ICR USING LINEAR AND NON-LINEAR REGRESSIONS

The main purpose of regression analysis is to obtain a mathematical relationship between one or more independent and dependent variables. Therefore, in the regression analysis, in addition to the correlation between the independent variables and the dependent variable being investigated, the type and form of the mathematical relationship are also determined [20-21]. In this study, in all linear and nonlinear regression models, the parameters of ICR, σ_t , σ_c ,

RQD, PCI, PCF, and SE were selected as input variables and instantaneous infiltration rate as output variable.

7.1. Linear Regression

In this study, to predict ICR, the correlation between independent and dependent variables was determined by Pearson's correlation coefficient (Table 6). Indeed, the correlation coefficient shows the severity of the linear relationship and the type of direct or inverse relationship between the independent and dependent variables.

Table 6. Pearson correlation coefficient matrix for parameters affecting the instantaneous drilling speed

Row	Variables	ICR	RQR	σ_t	UCS	RMBI	PCI	PCF	SE
1	ICR	1	-0.036	0.213	0.221	0.975	0.719	-0.934	0.220
2	RQD	-0.036	1	0.362	0.366	-0.640	-0.188	0.028	0.365
3	σ_t	0.213	0.362	1	1	0.176	0.199	-0.432	1
4	UCS	0.221	0.366	1	1	0.182	0.122	-0.438	1
5	RMBI	0.975	-0.064	0.176	0.180	1	0.831	-0.930	0.182
6	PCI	0.719	-0.188	0.119	0.117	0.831	1	-0.784	0.122
7	PCF	-0.934	0.028	-0.435	-0.435	-0.930	-0.784	1	-0.438
8	SE	0.220	0.365	1	1	0.182	0.122	0.438	1

To predict ICR, a multiple linear regression model was used with a simultaneous login method in which all independent variables were analyzed simultaneously. To perform linear regression, from 30 excavated sections in the tunnel, 22 sections were adopted for modeling, and 8 sections were selected for testing models. Based on these calculations, the linear regression equation for modeling was obtained as Eq. (7).

$$\begin{aligned}
 ICR = & 115.07 + 0.229(RQD) - 17.837(\sigma_t) \\
 & - 26.53(UCS) \\
 & - 7.47(RMBI) \\
 & + 0.034(PCI) \\
 & - 1.84(PCF) + 6.82(SE)
 \end{aligned} \quad (7)$$

To secure linear regression, the assumption of independence of errors, normal errors, and the linearity of independent variables should be tested. The Watson Camera Test can be used to

study the independence of errors. If the value of this statistic is in the range of 1.5–2, the assumption of the independence of errors can be considered. In addition, if the co-linear ratio is high in a regression equation, there is a high correlation between the independent variables. Therefore, despite the high coefficient of determination, the regression model may not have high credibility. The existence of this phenomenon can be examined by controlling the variance inflation factor (VIF) and tolerance. If VIF is more than 10 and the tolerance is less than 0.1, linearity between the independent variables is probable. If the VIF value is greater than 30, it indicates a serious problem. The coefficients of the regression model for the variables of research and control of the co-linear statistics of the model variables are shown in Table 7. The values of the VIF and table tolerance show that there is no coincidence between the variables included in this study.

Error frequency distribution charts and homogeneity of variances can also be plotted (Fig. 3). By comparing the error distribution diagram with the normal distribution diagram, it was found that the error distribution is almost normal because the mean value is close to zero and the

standard deviation is less than one. Regarding the homogeneity diagram of variances, a standardized dispersion curve of standardized residues versus fitting values shows the optimal state because the residues are randomly dispersed in a horizontal bar around a zero residual value (Fig. 4). Table 7 presents the statistical characteristics of the regression, analysis of variance, and regression coefficients. In Table 8, the ratio of F is 73.669 and is significant at the level of 0.001. Table 8 shows the statistical characteristics of the regression and variance analyses used to predict instantaneous drilling rates. The Durbin–Watson test is a test for examining the autocorrelation between residuals in structural and regression models. The Durbin–Watson statistic ranges from 0 to 4. If there is no sequential correlation between the residuals, the value of this statistic should be close to 2. If it is close to zero, it indicates a positive correlation, and if it is close to 4, it indicates a negative correlation. In general, if this statistic is between 1.5 and 2.5, it indicates favorable results [20]. Given that the Durbin–Watson statistic obtained is a number between 1.5 and 2.5, it therefore indicates favorable statistical results, and also because it is close to 2, it indicates positive correlation.

Table 7. Regression coefficients and their tests

Linear statistics		p-value	t-value	Standard	Non-standard coefficients		Model
				coefficients	Beta	Error level	
Tolerance	VIF	0.00	9.65	-----	11.92	115.07	Fixed
0.132	3.34	0.00	4.25	0.265	0.540	2.229	Qualitative Index of Rock Mass
0.379	3.33	0.00	3.25	-1.02	0.23	-17.837	Compressive resistance
0.533	4.45	0.007	-2.96	-1.38	8.95	-26.53	Tensile resistance
0.467	2.09	0.00	-6.98	-2.31	1.07	-7.47	Index of rock mass fracture
0.178	1.67	0.001	4.02	0.246	0.009	0.034	Blade consumption index
0.190	1.48	0.00	-9.67	-2.78	0.191	-1.84	Blade consumption factor
0.550	2.22	0.030	2.31	1.09	2.95	6.82	Special energy

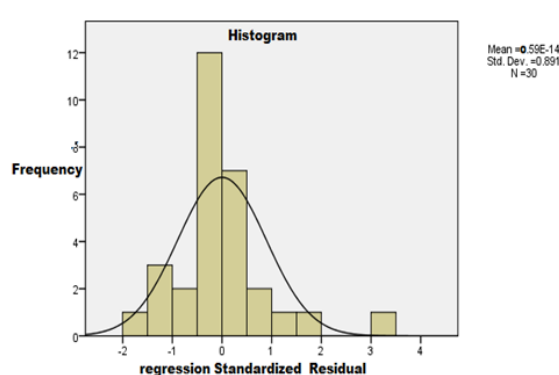


Fig. 3. Frequency distribution chart of errors.

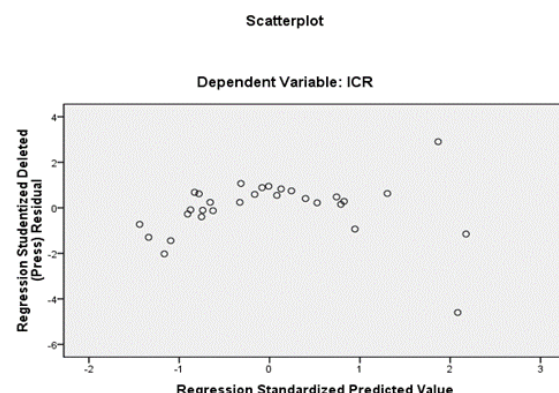


Fig. 4. Chart of homogeneity variances.

Table 8. Statistical characteristics of regression and variance analysis for predicting ICR

Model summary				
R	R2	Converted to R2	Standard error Estimation	Watson camera statistic
0.999	0.999	0.982	0.510	2.09
Variance analysis ANOVA				
Changes source	Sum of squares	Freedom degree	Mean of squares	Significance level
Regression	313.26	7	52.23	0.00
Remaining	0.266	23	0.021	-
Total	313.69	30	-	-

7.2. Multiple Nonlinear Regressions

In many cases, a linear model is used to determine the relationship between the independent and dependent variables. In fact, the relationship between variables is not always linear and may be non-linear. Therefore, in this study, the previous data were also fitted with polynomial, power, and exponential nonlinear models, which are discussed below [21].

A: Polynomial Nonlinear Regression

After the analysis, a polynomial model was used to predict the ICR of the road-header with a R-square (R^2) of 0.994 as Eq. (8).

$$\begin{aligned} ICR = & 46.170 + 0.051(RQD) - 61.176(\sigma_t)^2 \\ & + 0.005(UCS)^3 \\ & + 0.013(RMBI)^4 \\ & - 4.317(PCI)^5 \\ & - 4.906(PCF)^6 \\ & - 0.001(SE)^7 \end{aligned} \quad (8)$$

B: Power nonlinear regression

In this case, a nonlinear power regression model was used to forecast the ICR of the Roadheader with a R^2 of 0.997, as shown in Eq. (9).

$$\begin{aligned} ICR = & [1.540 - 1.867(RQD) - 0.237(\sigma_t) + 0.002(UCS) + \\ & 10.039(RMBI) - 0.002(PCI) - 0.003(PCF) + 0.060(SE)] \end{aligned} \quad (9)$$

C: Exponential nonlinear regression

A nonlinear exponential regression model was used to predict ICR of the Roadheader with a R^2 of 0.998, as shown in Eq. (10).

$$\begin{aligned} ICR = & \exp(-0.845 + 0.197(\sigma_t)^{-0.062} \\ & - 1.047(\sigma_t)^{0.716} \\ & + 0.076(UCS)^{0.280} \\ & + 1.566(RMBI)^{0.156} \\ & + 1.064(PCI)^{-0.041} \\ & + 1.972(PCF)^{-0.518} \\ & + 1.113(SE)^{0.439}) \end{aligned} \quad (10)$$

The relationship between the predicted values of ICR and the values measured by different models for the test data can be seen in Figures 4 to 6.

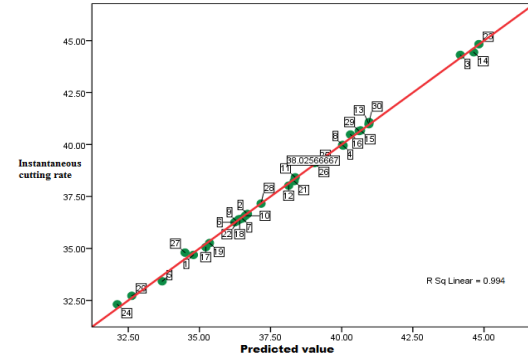


Fig. 4. Relationship ICR and its predicted values achieved by polynomial function ($R^2=0.994$).

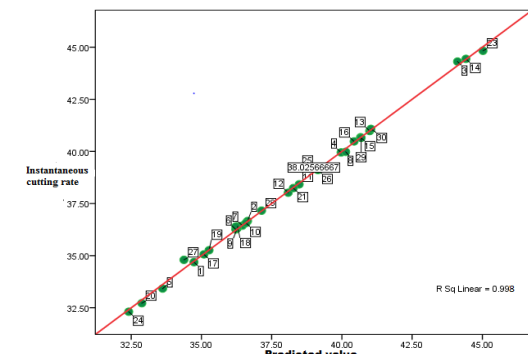


Fig. 5. Relationship between ICR and its predicted values achieved by exponential function ($R^2=0.998$).

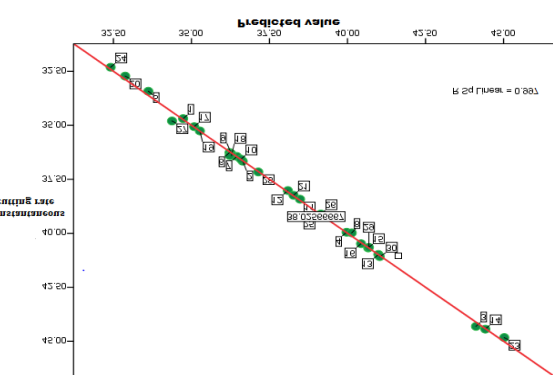


Fig. 6. Relationship between ICR and its predicted values achieved by power function ($R^2=0.998$).

8. SELECTING BEST MODEL FOR ALGORITHM POS

To evaluate the performance of different models, compare them, and choose the best model, R^2 , square root mean square of errors, mean absolute percentage error (MAPE), and VAF are determined for each model. The results show that there is a good relationship between the instantaneous drilling rate of the Roadheader and the predicted value of the parameters with a very high R^2 of the exponential functions model ($R^2 = 0.998$). To select the best model for estimating the drilling rate of the Roadheader machine, based on nonlinear and linear regression models, the linear regression model with the highest R^2 , i.e., the value ($R^2=0.999$) was selected. To obtain the best model among 30 sections, we selected and calculated 8 sections for the predicted value and 22 sections for the measured value. Table 9 shows the best model for the PSO algorithm based on the determined effective factors.

Table 9. Selection of the best model for the PSO algorithm based on the determined effective factors

Model	R^2	RMSE	MAPE	VAF
Linear regression	0.999	0.612	0.07212	99.80
Nonlinear regression of polynomial function	0.994	0.985	0.07717	86.1
Nonlinear regression of power function	0.997	0.885	0.07814	87.1
Nonlinear regression of exponential function	0.997	0.945	0.07316	88.1

9. OPTIMIZATION OF ICR USING THE ALGORITHM PSO (PARTICLE MASS OPTIMIZATION ALGORITHM)

Selecting the appropriate input parameters is an important part of evolutionary intelligence algorithms and analytical models. Using the analysis of the main components, we can determine the parameters affecting a physical phenomenon. In this research, the input and output parameters for 30 considered sections as the case study are RQD, UCS, σ_t , RMBI, PCI, PCF, SE, as input parameters, and ICR as the output parameter.

To model the issue, all the values of the parameters must be recorded so that they can be called up from the function when needed. At this stage, the definition and implementation of the initial values are performed as shown in Figure 8.

In this section, we specify the target function, the number of unknown variables, the structure of the unknown variables, and the upper and lower limits of the variables. The relationship obtained

from the linear regression model was used to predict the ICR in the PSO algorithm. The linear regression model was implemented several times with parameter variations. This trend continued until the algorithm reached the appropriate convergence. The target function is ICR. According to Figure 7, the results of the PSO algorithm show that to obtain the optimum level of the target function for a rock section with a σ_t of 51.78 MPa and a RQD of 33.09%, ICR of the Roadheader is equal to 36.41 m³/h. In Figure 8, the horizontal axis represents the number of function evaluations or NFEs.

```

1 function model=CreateModel()
2
3 %UCS=33.567+0.223*RQD-17.837*sigma_t-36.53*RMBI+0.034*PCI-1.84*PCF+6.82*SE
4
5 %RQD=33.09, UCS=38.16, sigma_t=51.78, RMBI=22.60, PCI=5.61, PCF=7.34, SE=0.01
6
7 gmax=33.09; lmin=1.53; rmax=38.16; lmin2=1.22; rmax2=22.60; lmin3=5.61; rmax3=7.34
8
9 j1=gmax*33.09; lmin3=gmax*1.53; rmax3=gmax*38.16; lmin2=gmax*1.22; rmax2=gmax*22.60; lmin=gmax*5.61; rmax=gmax*7.34
10
11 j2=gmax*35.46; lmin2=gmax*2.37; rmax2=gmax*51.78; lmin3=gmax*5.37; rmax3=gmax*11.14; lmin=gmax*11.04; rmax=gmax*7.34
12
13 j3=gmax*35.46; lmin=gmax*2.37; rmax=gmax*51.78; lmin3=gmax*5.37; rmax3=gmax*11.14; lmin2=gmax*11.04; rmax2=gmax*7.34
14
15
16 %RQD=[11.07 0 0 0 0 0];
17 %UCS=[22.79 17.837 26.53 7.67 0.034 1.84 6.82];
18 %sigma_t=[0 0 0 0 0 0];
19
20 %model=fmincon(@f,[RQD;UCS;sigma_t;RMBI;PCI;PCF;SE],lb,ub,A,b,Aeq,beq,lb,ub);
21
22 %fmincon(f,x0,lb,ub,A,b,Aeq,beq,lb,ub);
23
24 model=lsqnonlin(@f,[RQD;UCS;sigma_t;RMBI;PCI;PCF;SE],lb,ub,A,b,Aeq,beq,lb,ub);
25 model=lsqnonlin(@f,[RQD;UCS;sigma_t;RMBI;PCI;PCF;SE],lb,ub,A,b,Aeq,beq,lb,ub);
26 model=lsqnonlin(@f,[RQD;UCS;sigma_t;RMBI;PCI;PCF;SE],lb,ub,A,b,Aeq,beq,lb,ub);
27 model=lsqnonlin(@f,[RQD;UCS;sigma_t;RMBI;PCI;PCF;SE],lb,ub,A,b,Aeq,beq,lb,ub);
28 model=lsqnonlin(@f,[RQD;UCS;sigma_t;RMBI;PCI;PCF;SE],lb,ub,A,b,Aeq,beq,lb,ub);
29 model=lsqnonlin(@f,[RQD;UCS;sigma_t;RMBI;PCI;PCF;SE],lb,ub,A,b,Aeq,beq,lb,ub);
30 model=lsqnonlin(@f,[RQD;UCS;sigma_t;RMBI;PCI;PCF;SE],lb,ub,A,b,Aeq,beq,lb,ub);
31
32 end

```

Fig. 7. Modeling of input parameters for optimization of the considered tunnel.

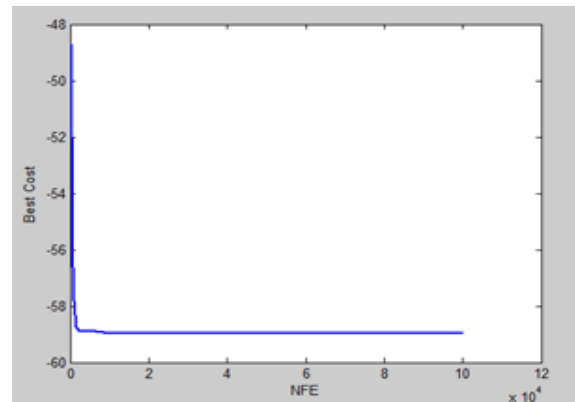


Fig. 8. Output of optimization issue of ICR of Roadheader as a diagram.

10. ANALYZING THE SENSITIVITY OF THE NEURAL NETWORK MODEL USING THE COSINE FIELD METHOD

Sensitivity analysis is the study of the effect of output variables on the input variables of a statistical model. In other words, it is a way to change the inputs of a systematic statistical model that can predict the effects of these changes in the output of the model. The cosine field method is used to determine the ratio between the involved parameters. In this section, the intensity of the relationship between the ICR and the input

parameters is determined. The results are illustrated in Table 10.

Table 10. Analysis of the sensitivity of the input parameter model to the instantaneous drilling rate using the cosine field method

Input parameter	Sensitivity level to the instantaneous drilling rate
Qualitative index of rock mass (%)	0.999
Tensile resistance (MPa) (σ_t)	0.996
Single-axial compressive resistance of the rock (UCS) (MPa)	0.997
Fragility index of the rock mass (RMBI)	0.995
Partition consumption index (PCI)	0.995
Partition consumption factor (PCF)(m ³ /pick)	0.997
Specific energy (SE) (MJ/M3)	0.992

As shown in Figure 9, σ_t , UCS, RQD, and PCF are the most important parameters affecting ICR. In addition, the influence of RMBI is relatively strong. Parameters such as SE and PCI are more sensitive to input parameters than ICR.

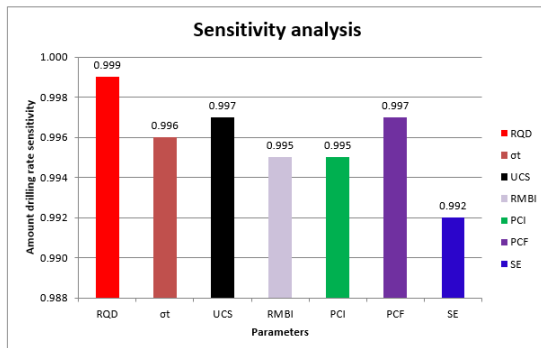


Fig. 9. Intensity level of the instantaneous drilling rate relationship with each input parameter.

According to Table 10, the results were analyzed by SPSS Software to measure the intensity level of ICR relationship with each of the input parameters.

The effective parameters in determining ICR for the case study were evaluated by cosine field sensitivity analysis, which are as follows:

A: The computational error rate is almost zero, indicating that the trained network has reached the desired convergence.

B: The rate of advancement for these tunnels from the input parameters is strongly influenced by the geomechanically properties of the rock.

11. CONCLUSION

This research presented a model to predict the performance of Roadheader machine in underground coal mines based on characteristics

and geotechnical parameters of rock. In this regard, a case study including 30 sections along a tunnel in Parvadeh No. 1 underground coal mine was taken to account. Analyses were performed based on linear regression and nonlinear regression, and the ANF system to predict instantaneous cutting rate (ICR) of Roadheader. Based on the introduced approach, prediction of ICR in various geotechnical conditions is available for tunnels and roadways in underground coal mines. The prediction was conducted using the neural network and PSO algorithm. The best linear regression model was selected according to the performance evaluation methods. To achieve the best model made by the neural network, the coefficient of determination (R^2), performance index, root mean square error, and mean absolute error percentage were used. Finally, to select the best model for estimating ICR, the linear regression system has a better estimation and higher accuracy than nonlinear regression. The mean squared error for the linear regression model is less than that for the other two models, and the correlation coefficient in linear regression is greater than that in nonlinear regression. This is while linear regression has a determination coefficient $R^2 = 0/999$, and this value has tremendous reliability. Finally, by inserting the linear regression results in the PSO algorithm, it is shown that to obtain the optimum target function for the rock mass transfer with a UCS of 1.68 MPa and RQD of 33.09%, ICR of the Roadheader equals 33.11 cubic meters per hour. Considering specific energy (SE) as an important parameter in determining the drilling rate, so this parameter should be considered for determination of ICR. Here, the results of the algorithm show that for 34.21 of the consumable partition, SE should be 6.15 MJ/m³.

REFERENCES

- [1] Ebrahim Abadi, A. (2012). Introducing a Model for Road headers' Performance Prediction Based on the Specific Energy and the Angle between Tunnel Axis, Quarterly Scientific - Research Journal of Environmental Geology, Year 6, Issue 20 - Shap 2008-4250.
- [2] Ebrahimabadi, A., Goshtasbi, K., Shahriar, K., and Cherghi, Seifabad, M. (2011). Predictive Models for Roadheaders' Cutting Performance in Coal Measure Rocks", YERBILIMLERI Journal, Vol. 32, No. 2, pp 89-104.
- [3] Ebrahimabadi, A. (2012). Stability Analysis and Optimum Support Design of Tunnel No. 1 of Central Mine in Tabas Coal Mine Project", ITA-AITES World Tunnel Congress and 38th General Assembly (2012), Bangkok, Thailand, 8p.

[4] Ebrahimabadi, A., Azimipour, A and Bahreini, A. (2016). Prediction of Roadheaders' performance using artificial neural network approaches (MLP and KOSFM)", *Tunneling and Underground Space Technology*, Volume 59, Pages 127-133.

[5] Comakli, R., Sair Kahraman, S and Balci, C., (2014). Performance prediction of Roadheaders in metallic ore excavation", *Tunneling and Underground Space Technology*, 38-45.

[6] Bilgin, N. and Ocak, I. (2010). Comparative studies on the performance of a Roadheader, impact hammer and drilling and blasting method in the excavation of metro station tunnels in Istanbul", *Tunnelling and Underground Space Technology*, Volume 25, Issue 2, Pages 181-187.

[7] Bilgin, N., Dincer, T., Copur, H and Erdogan, M. (2004). Some Geological and Geotechnical Factors Affecting the Performance of a Roadheader in an Inclined Tunnel", *Tunnelling and Underground Space Technology*, Vol 19, Elsevier, pp. 629-636.

[8] Eftekhari, S. M. and Bastami, M. (2020). Effect of the Replacement of Cutting Tools on the Performance of TBM in Tehran Metro Line 6. *Journal of Analytical and Numerical Methods in Mining Engineering*, 10(24), 63-76. doi: [10.29252/annm.2020.13703.1438](https://doi.org/10.29252/annm.2020.13703.1438).

[9] Mokhtarian, M. , Eftekhari, M. and Baghbanan, A. (2014). Application of Principal Component Analysis in Prediction of Penetration Rate of TBM Using Artificial Neural Networks. *Journal of Analytical and Numerical Methods in Mining Engineering*, 3(6), 33-43.

[10] Khodaee Ashestani, S. , Chakeri, H. , Darbor, M. , Khoshzaher, E. and Bazargan, S. S. E. (2023). Estimating Penetration Rate of Excavation Machine Using Geotechnical Parameters and Neural Networks in Tabriz Metro. *Journal of Analytical and Numerical Methods in Mining Engineering*, 13(37), 1-9. doi: [10.22034/annm.2023.20414.1604](https://doi.org/10.22034/annm.2023.20414.1604).

[11] Bilgin, N and Balci, C. (2005). Performance Prediction of Mechanical Excavators in Tunnels, Training Course of Tunnel Engineering, Istanbul Technical University, Turkey.

[12] Copur, H., Ozdemir, L and Rostami, J. (1998), "Roadheader Applications in Mining and Tunneling Industries", The Mining Engineering, pp. 38-42.

[13] Hosseini, A. , Najafi, M. and morshedy, A. H. (2022). The effect of technical parameters of cross-measure boreholes methane drainage method on the amount of exhaust gas (Case study: Tabas Parvadeh coal mine No.1). *Journal of Analytical and Numerical Methods in Mining Engineering*, 12(30), 79-89. doi: [10.22034/annm.2022.2570](https://doi.org/10.22034/annm.2022.2570).

[14] Hosseini A, Najafi M (2021) Determination of Methane Desorption Zone for the design of a drainage borehole Pattern (Case Study: E4 Panel of the Tabas Mechanized Coal Mine, Iran). *Rud Zb* 36:61-75.

[15] Hosseini A, Najafi, M and Morshedy, AH. (2022) Determination of suitable distance between methane drainage stations in Tabas mechanized coal mine (Iran) based on theoretical calculations and field investigation. *J Min Inst* 258:1050-1060.

[16] Hosseini, A., Najafi, M., Shojaathosseini, SA and Rafiee, R. (2017) Determination of a suitable extraction equipment in mechanized longwall mining in steeply inclined coal seams using fuzzy analytical hierarchy method (Case study: Hamkar coal mine, Iran). *J Min Environ* 8:487-499.

[17] Dosco Overseas Engineering Ltd, (2008), Newark Nottinghamshire, England, www.dosco.co.uk.

[18] Rostami, J., Ozdemir, L and Neil, D., M. (1994), "Roadheader Performance Optimization for Mining and Civil Construction", Proceedings of 13th Annual Technical Meeting of the Institute of Shaft Drilling Technology (ISDT), Las Vegas, pp. 1-17.

[19] Thuro, K and Plinninger, R.J. (1999), "Roadheader Excavation Performance - Geological and Geotechnical Influences", 9th ISRM Congress Paris, Theme 3: Rock Dynamics and Tectonophysics/Rock Cutting and Drilling, pp.25-28.

[20] Mostowfi, N. (2011), learn how to use MATLAB", Department of Chemical Engineering, Tehran University.

[21] B. H. G. Brady and E. T. Brown, (1993), "Rock Mechanics for Underground Mining", Second Edition.

[22] S. Hamekhoni, and Ramzan Ali Royaei, (2022), The Effect of Cultural Factors on Cost Stickiness, Financial Accounting and Auditing Research, Volume 14, Number 54, Pages 159-178.